

Baden-Württemberg Stiftung
"Research" Series: No. 56

Nanotechnology – Fundamentals and Applications of Functional Nanostructures

Th. Schimmel, H. v. Löhneysen, M. Barczewski



A programme of the

**BADEN-
WÜRTTEMBERG**
STIFTUNG 
Wir stiften Zukunft

Cover: Au nanostructures produced by a printing process based on block-copolymer templating. The line width and distance are ~50 nm. The mesh-like structures around the line pattern stem from the inherent block-copolymer morphology.

T. Heiler, R. Gröger, S. Walheim, Th. Schimmel;
Karlsruhe Institute of Technology (KIT)

Nanotechnology – Fundamentals and Applications of Functional Nanostructures

Results of the second research programme Kompetenznetz “Funktionelle Nanostrukturen” (Competence Network on Functional Nanostructures)

Publisher

Baden-Württemberg Stiftung gGmbH,
Im Kaisemer 1, 70191 Stuttgart

Prof. Dr. Thomas Schimmel, Prof. Dr. Hilbert v. Löhneysen,
Dr. Matthias Barczewski

Liability

Rudi Beer (Director Research and Science, Baden-Württemberg Stiftung)

Design and Layout

Dr. Matthias Barczewski

Photos

All photos contributed by the authors of the articles.

Printing

E&B engelhardt und bauer, Käppelestraße 10, 76131 Karlsruhe

© Baden-Württemberg Stiftung, April 2011

ISSN 1610-4269

ISBN 978-3-00-030810-9

Localized ATP synthesis to control a biological nanomotor

M. Börsch¹, P. Gräber², J. Heinze³, J. Wrachtrup¹

¹ 3. Physikalisches Institut, Universität Stuttgart, Pfaffenwaldring 57, 70550 Stuttgart

² Institut für Physikalische Chemie, Universität Freiburg, Albertstr.23 a, 79104 Freiburg

³ Freiburger Materialforschungszentrum FMF, Universität Freiburg, Stefan-Meier-Str. 21, 79104 Freiburg

Summary

The enzyme H⁺-ATP synthase (F₀F₁-ATP synthase) couples two internal motors mechanically. We bind two markers to the enzyme to observe rotation of the two motors, that is, the ATP-driven F₁ motor with three 120° steps as well as the proton-driven F₀ motor with 10 substeps. The continuous distance monitoring between the two markers is accomplished by fluorescence resonance energy transfer (FRET) in a single, liposome-embedded H⁺-ATP synthase. The distance changes in the nanometer range determine the step size of the processes. New fluorophores (CdSe quantum dots, fluorescent nanodiamonds and photostabile perylene) were evaluated to reveal the step size of 36° during rotation of the proton-driven F₀ motor for the first time, that is, 10 single steps per full rotation.

Using our “duty cycle- optimized alternating laser excitation” approach we proved that both FRET donor fluorophore and FRET acceptor fluorophore were present in each single molecule. Thus, spectral fluctuations of the FRET donor causing FRET artifacts in single-molecule detection were minimized. To extract distances and the respective changes within a single molecule in an unbiased way, we developed a new software-based data analysis method using Hidden Markov Models (HMM). HMMs can be applied to F₀ motor studies as well as ATP-driven rotation within the F₁ motor utilized to determine the local ATP concentration. ATP-dependent rotation was measured by video microscopy using nano particles (nanodiamonds or polystyrene beads) bound to the γ subunit in surface-attached F₁-parts.

To control the H⁺-ATP synthase we have combined confocal microscopy with three-dimensional positioning of a nanoelectrode. Thus, the local pH can be adjusted by a chemical reaction at the tip of the nanoelectrode. Alternatively, we have evaluated optical traps for proteoliposomes to turn on ATP synthesis spatially.

1 Introduction

Enzymes are the biological nanomachines which catalyze chemical reactions at ambient temperatures. They work in every cell and many use an ubiquitous small molecule adenosine triphosphate (ATP) as the energy currency. Biological transporters like myosins and kinesin as well as ion pumps use ATP to move cargo against a concentration gradient or unidirectionally against random Brownian motion. The usable energy in ATP is stored in the terminal ester bond, which gets hydrolyzed and the released products are ADP (adenosine diphosphate) and phosphate. A human organism needs about 70 kg ATP per day and, therefore, ATP cannot be taken up by eating. Instead, the hydrolysis products ADP and phosphate have to be recycled within each cell or organism. The machine which accomplishes this formation of ATP from ADP and phosphates is called F_0F_1 -ATP synthase (H^+ -ATP synthase).

F_0F_1 -ATP synthases are large multi subunit enzymes in the membranes of bacteria, the inner mitochondrial membranes or in the thylacoid membranes of plant cells, respectively. The F_0F_1 -ATP synthases are about 20 nm in height and 5 to 10 nm in diameter[1]. In general, they consist of the protruding F_1 part with the three catalytic binding sites for ATP, ADP and phosphate, and the F_0 part which is embedded in the lipid membrane. The total number of subunits is depending on the organism. For the bacterial enzyme from *Escherichia coli*, the F_1 part consists of five different subunits with the stoichiometry $\alpha_3\beta_3\gamma\delta\epsilon$. The F_0 part comprises subunits ab_2c_{10} . The driving force for ATP synthesis by the *E. coli* F_0F_1 -ATP synthase is an electrochemical potential difference of protons across the membrane[2]. How is the Gibbs free energy as the driving force transduced to the chemical synthesis reaction within the enzyme? Conformational changes in the catalytic nucleotide binding sites alter the binding affinities of substrates and products as proposed by the "binding change mechanism"[3], and the conformational changes are induced by mechanical movements.

F_0F_1 -ATP synthases are rotary motors, and each of the two parts is a rotary nanomotor by itself[4, 5]. Both motors are directly connected, but drive the opposite direction of the catalytic reaction between ATP and ADP plus phosphate[6–9]. Hydrolysis of ATP produces torque in the F_1 motor, which is accomplished by a very high conversion efficiency of chemical into mechanical energy[10]. The efficiency approaches 100 percent. The rotary motion of the ATP-driven F_1 motor was demonstrated biochemically[11], using fluorescence anisotropy[12], and, most convincingly, by video microscopy of single surface-bound F_1 [10]. Therefore, fluorescent μm -long actin filaments or polystyrene beads were attached as markers to the rotating γ subunit in F_1 . At high ATP concentrations, i.e. in the millimolar range, the γ subunit rotated in 120° steps.

However, at low ATP concentrations, three additional stopping positions of the rotor were identified[13]. The rotational speed for a 360° turn was strictly related to the ATP concentration, and, *vice versa*, measuring rotation can be used as a read-out for the local ATP concentration.

In contrast, the F_0 motor is a turbine which is driven by proton flow. The a subunit provides an inlet and an outlet half-channel for the protons, and the protons are transferred one after another to a binding site on each c subunit. Rotation of the c ring is induced by the reversible compensation of charges at the a - c interface[14]. This results in a Brownian ratchet mechanism for the unidirectional rotation which is required to drive ATP synthesis[15]. The mechanical transducer to the ATP binding sites in F_1 is the central stalk between the two motors which is built by the γ and ϵ subunit of F_1 interfacing the ring of c subunits of F_0 . According to the model, the c ring rotates in 10 small steps, at least during during proton-driven ATP synthesis. However, the γ and ϵ subunit rotate in 120° steps during ATP synthesis. The question has to be answered where the elastic energy is stored transiently to overcome this symmetry mismatch problem. Therefore we aimed at measuring the step size of the c ring in single F_0F_1 -ATP synthase during proton-driven ATP synthesis.

F_0F_1 -ATP synthase is a self-assembled motor complex which is about three orders of magnitude smaller than man-made mechanical devices. From a nanotechnological point of view for applications of this rotary nanomotor, it will be essential to understand how the self-assembly process occurs, what the principles of the motor operation are, how the extraordinary efficiency of energy conversion is achieved, how genetical modifications affect the torque and the stability of the complex, how stable the motor works in different environments (pH, solvents, and temperature) and how the ATP synthesis reaction can be optimized. Then, driving other biological linear nanomotors on their respective biological railway systems might become real by controlling a localized ATP production as the fuel, and new biomimetic cargo transport systems might be established on the nanometer scale.

2 Results and Discussion

2.1 Single-molecule fluorescence resonance energy transfer for rotation measurements in F_0F_1 -ATP synthase

We have developed a spectroscopic tool to monitor the rotary motion of each of the two motors in a single F_0F_1 -ATP synthase. Since 2001, we use two fluorescent dye molecules attached to different parts of the F_0F_1 -ATP synthases [16]. After genetical introduction of reactive amino acids, i.e. cysteines, these positions on the rotor or the stator can be labeled specifically with commercially available dyes. Alternatively, we used autofluorescent proteins fused to the proton-translocating α subunit in F_0 [17, 8]. We also evaluated labeling a reactive lysine (residue 4) on the static β subunits in F_1 and an off-axis position at the rotating γ subunit (residue γ 106) [18]. Because both fluorophores are positioned off-axis, the motion of the fluorophore at the rotor subunit causes changes in the relative distance to the second fluorophore. The distances are measured with millisecond time resolution using the Förster-type resonance energy transfer, FRET. FRET is based on radiation-less energy transfer due to the spectral overlap of the two fluorophores. For example, the emission spectrum of the FRET donor partly overlaps with the absorption of the FRET acceptor fluorophore. The FRET efficiency is distance dependent with r_{DA}^{-6} (with r_{DA} , distance between the donor and acceptor fluorophore). For different distances, FRET can be varied by the spectral properties of the two dyes and their relative orientation or mobilities, respectively. To optimize the sensitivity for small distance changes as expected for the rotary motions in F_0F_1 -ATP synthase, several pairs of fluorophores with different Förster radii R_0 for 50 percent energy transfer had to be evaluated. Using the FRET pair EGFP (enhanced green fluorescent protein, FRET donor with low fluorescence quantum yield) and Alexa568 yielded a small $R_0 = 4.9$ nm [8], and with the FRET pair sulforhodamine B and Cy5 we used a large $R_0 = 8.2$ nm due to an enhanced spectral overlap [18]. SulforhodamineB/Cy5 were chosen to monitor rotation via FRET from a position on the top of F_1 to the bottom spanning about 10 nm.

To observe individual single F_0F_1 -ATP synthases during rotation, a custom-designed confocal microscope was built. Focussing the laser by a microscope objective with high numerical aperture resulted in a nearly diffraction-limited laser spot for the excitation of the fluorophores. The volume of this spot was adjusted to 5–10 fl. Diluting the FRET-labeled F_0F_1 -ATP synthases to concentrations below 1 nM yielded a mean of less than one enzyme in the laser focus at any time. This principle of single-molecule detection in an open volume, that is in a droplet of buffer solution, allows for observation of conformational states during the transit time of the freely diffusing enzyme. The transit time

of a single F_0F_1 -ATP synthase with a molecular weight of 560 kDa is prolonged due to the reconstitution (i.e. functional embedding) into a lipid vesicle of 100–150 nm diameter. These proteoliposomes remained in the laser focus for up to several hundred milliseconds, which is sufficiently long to observe not only one single conformation or orientation of the rotor subunit, but for many subsequent orientations, if the rotation is fast and the dwell times for each conformation are in the range of 10 to 100 milliseconds. ATP-driven rotation at 1 mM ATP resulted in mean dwell times of more than 10 ms. The dwell times of proton-driven rotation of γ and ϵ were found between 12 and 52 ms. Accordingly, turnover rates of F_0F_1 -ATP synthase at room temperature perfectly matched the observation time intervals of the single-molecule detection scheme using freely diffusing proteoliposomes.

The identification of a specific conformational state or relative orientation of the rotor subunit in F_0F_1 -ATP synthase is achieved by measuring the distance using the fluorescence intensities of FRET donor and acceptor. As long as the FRET efficiency deviations from the mean level are small, that is, remain in the distance range of less than 0.5 nm per data point, these data points in the fluorescence time trajectory are associated with the same conformation or orientation. Once the deviations are larger, a new conformation is defined. Using fluorescence lifetime information in parallel with picosecond pulsed lasers, the FRET efficiency can be calculated independently from intensities [17, 19]. Thus, FRET artifacts due to reversible quenching of donor or acceptor fluorophores (“blinking”) can be minimized. However, spectral fluctuations cannot be eliminated, and biochemical controls of the F_0F_1 -ATP synthase activities are needed to extract the correct dwell times and to resolve orientations and the step sizes of the different rotor subunits.

2.2 Labeling F_0F_1 -ATP synthase with quantum dots

The photostability of the organic dye molecules used for the FRET measurements of a single F_0F_1 -ATP synthase limited the applied laser excitation power and, therefore, the signal-to-noise ratio. Luminescent semiconductor nanocrystals (quantum dots, QD) have unique photophysical properties like high photostability and narrow, size-tunable fluorescence spectra. Quantum dots with hydrophilic shells are commercially available. However, a strong blinking effect, i.e. an intermittance of fluorescence, impairs the use as FRET fluorophores. In addition, the size of some quantum dots including the hydrophilic shells reaches 20–40 nm, that is, even larger than the F_0F_1 -ATP synthase, which might affect the conformational dynamics of the enzyme.

The small CdSe/ZnS quantum dot QD490 with an amino-modified surface resulting in an effective diameter of 11 nm was evaluated as a potential FRET

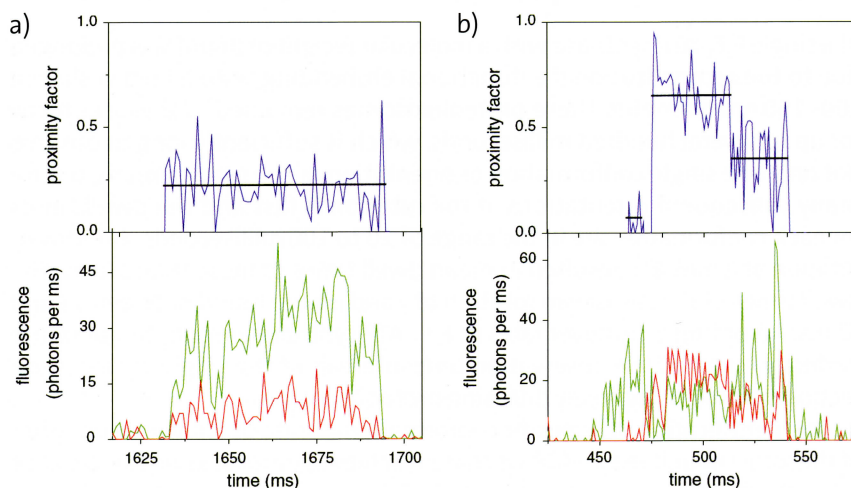


Fig. 1: Photon bursts from single FRET-labeled F_0F_1 -ATP synthases with a quantum dot QD490 as FRET donor on the static b subunits, and Alexa568 as FRET acceptor at the rotating ϵ subunit. The enzymes were integrated in liposome membranes ([21], excitation at 476 nm). Lower panels show FRET donor intensities I_D from QD490 (green traces) and FRET acceptor intensities I_A from Alexa568 (red traces). Upper panels show the corresponding proximity factor $P=I_A/(I_A+I_D)$ as blue traces. The mean proximity factor is shown as a black line. (a) Photon burst in the absence of ATP. (b) Photon burst in the presence of 1 mM ATP.

donor. After chemical derivatization to a maleimide, QD490 was attached selectively at cysteines to the peripheral, non-rotating b subunits (residue position 64) of the F_0 part[20, 21]. Labeling efficiency of the b subunits was calculated to 90%. ATP synthesis activity of the QD490-labeled enzyme was only slightly decreased to about 75%. To obtain the FRET-labeled enzyme, Alexa568 was used as the FRET acceptor and bound to the rotary ϵ subunit (residue 56) in the F_1 part. Fluorescence measurements in cuvettes of the double-labeled F_0F_1 -ATP synthase in liposomes clearly showed FRET following excitation at 476 nm.

In confocal single-molecule detection, the diffusion of the FRET-labeled proteoliposomes through the laser focus resulted in the expected photon bursts showing fluorescence in the FRET donor and FRET acceptor detection channels[21]. As shown in Fig. 1a, the ratiometric proximity factor $P=I_A/(I_A+I_D)$ or the FRET efficiency, respectively, remained constant in the absence of ATP indicating no rotational movement of the ϵ subunit. Several hundred enzymes were analyzed and three distinct FRET efficiencies were found. During ATP hydrolysis in the presence of 1 mM ATP, fluctuations of the FRET efficiency within a single photon burst indicated the stepwise rotational motion of the

ϵ subunit (Fig. 1b). Three transient orientations of the ϵ subunit were observed which could be related to 120° stepping of ϵ . For about 80% of the photon bursts, the sequence of FRET efficiency changes was found in the order of low \rightarrow high \rightarrow medium \rightarrow low \rightarrow . This corresponds to the sequence found earlier in single-molecule FRET measurements using Cy5 (FRET acceptor) to crosslink the two b subunits and tetramethylrhodamine as the FRET donor on the ϵ subunit. We conclude that the QD490 is bound similarly and symmetrically between the two b subunits. Due to the hydrophilic shell, the actual size of the fluorescent quantum dot is much larger than the size of an organic fluorophore. This affects the possibility of exact distance measurements.

The brightness of the single quantum dot, which was measured as the maximal photon count rate per ms, was not changed after covalent binding to the F_0F_1 -ATP synthase. Single quantum dots and QD490-labeled F_0F_1 -ATP synthases were attached nonspecifically to the cover glass and excited by total internal reflection microscopy. In contrast to the un-reacted quantum dots, the cysteine-bound nanocrystals exhibited drastically reduced blinking and stable fluorescence for several seconds.

Alternatively, rotational movements in single enzymes can be measured using fluorescence anisotropy properties of the quantum dot. It was possible to detect subunit rotation of the detergent-solubilized F_0F_1 -ATP synthase with a QD490 bound to the c -ring of the F_0 part [20]. Using confocal microscopy, stable fluorescence anisotropy was found in the absence of ATP. During ATP hydrolysis the fluorescence anisotropy of the quantum dot changed stepwise presumably indicating ATP-driven rotation. However, by anisotropy measurements we could only distinguish between transition dipole orientations between 0° and 90° for symmetry reasons.

2.3 Monitoring the F_0 motor step size

Having established the 120° step size of the rotor subunits γ and ϵ in the proton-driven F_0F_1 -ATP synthase during ATP synthesis we aimed at determining the step size of the c -ring in the F_0 part. We attached one fluorophore at the non-rotating a subunit and the second fluorophore to one of the 10 c subunits. To label the a subunit, a fluorescent protein (EGFP) was fused to the C terminus *via* a short, four amino acid linker. Accordingly each F_0F_1 -ATP synthase contained the FRET donor fluorophore on subunit a . *In vivo* imaging of the *E. coli* cells revealed the localization of EGFP on the membranes and not in inclusion bodies within the *E. coli* [8]. Because our plasmid construct did not overexpress the F_0F_1 -ATP synthase strongly, a microscopic localization within the plasma membrane supports the assumption of a functional mutant enzyme capable of ATP synthesis.

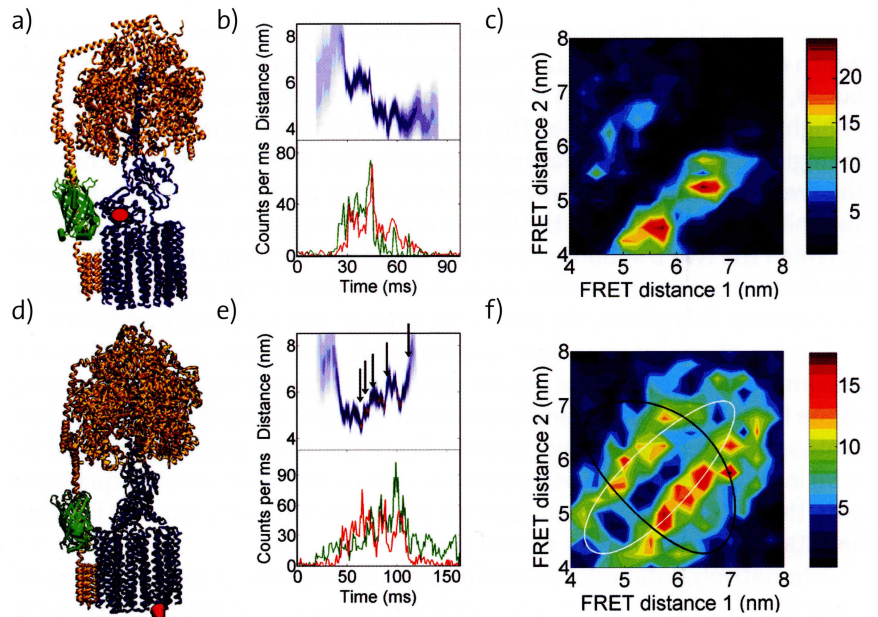


Fig. 2: Subunit rotation in F_0F_1 -ATP synthase monitored by single-molecule FRET. The blue subunits comprise the rotor, the orange-colored the stator. (a) FRET donor EGFP (green) is fused to the static a subunit, and FRET acceptor Alexa568 (red dot) to the rotating e subunit[8]. (b) Single photon burst showing 120° stepwise distance changes (blue trace) between a and e. Three main FRET distances are found. (c) FRET transition density plot for e rotation with three stopping positions for the rotating e subunit. (d) The FRET acceptor is attached to one c subunit (red dot) to observe c-ring rotation[19, 22]. (e) Multiple subsequent steps (black arrows) occur during c rotation upon ATP synthesis. (f) FRET transition density plot for c rotation indicating 36° step size (white circle) and not 120° steps (black circle).

At first the three-dimensional position of the C terminus within a single F_0F_1 -ATP synthase was unraveled by single-molecule FRET triangulation[8]. The FRET acceptor fluorophore Alexa568 was bound to the ϵ subunit at position 56, which was shown previously to rotate in 120° steps during ATP hydrolysis and synthesis. During stepwise rotation of ϵ three distinct distances were found as shown in Fig. 2b. When the pairs of subsequent FRET distances are plotted, that is, FRET distance 1 versus FRET distance 2 in Fig. 2c, three main transitions can be identified. In addition the order (or direction of rotation) of FRET transitions is directly accessible from the FRET transition density plot. Relating the slightly different dwell times for each of the ϵ orientations to previous single-molecule FRET measurements with the second fluorophore on the b subunits, it is possible to triangulate the EGFP position in the model

of *E. coli* ATP synthase. Due to the geometrical constraints given by the model structure, measuring a single F_0F_1 -ATP synthase showing three rotary steps of ϵ during the transit time in the laser focus is sufficient to triangulate the EGFP position in less than 100 ms. Accordingly, the C terminus of subunit *a* is located to the right hand side of the *b* subunit dimer, and the EGFP position is found near to the cytosolic membrane plane towards the F_1 part. Thus, the *a* subunit mechanically stabilizes the peripheral stalk by pushing the *b* dimer for both catalytic conditions, ATP hydrolysis and ATP synthesis.

With the known position of the EGFP label on the C terminus of *a*, the single-molecule FRET measurements of the rotating *c* subunits could be analyzed quantitatively (see Fig. 2d). During proton-driven ATP synthesis, several short FRET levels were found in photon bursts of single F_0F_1 -ATP synthase[22]. Obviously more than three distinct levels occurred (Fig. 2e). However, due to the low fluorescence quantum yield of EGFP, the position of the FRET levels and the transitions between them were sometimes difficult to determine by the manual data analysis approach. Therefore we applied objective criteria (that is, minimum number of photons per FRET level, limited variance within each FRET level) to select only the non-ambiguous transitions. These FRET transitions were plotted pairwise in the FRET transition density plot shown in Fig. 2f. Most of all absolute distance changes were found to be smaller than 1 nm indicating small rotary steps. Calculating the possible FRET transitions for 120° for each possibly labeled *c* subunit resulted in the black curve in Fig. 2f. *Vice versa*, calculating the FRET transitions for a 36° step size of *c* yielded the white theoretical curve in Fig. 2f. About half of the measured FRET transitions were associated with the 36° stepping model, and, additionally, up to 40% were interpreted as two subsequent 36° steps, that is apparent 72° steps, as anticipated for fast stepping of the *c*-ring and thus missing a short intermediary step.

EGFP photophysics and low fluorescence quantum yield hampered the FRET analysis of *c*-ring rotation. To prove the 36° step size of the *c*-ring, we developed a distinct FRET approach with different FRET fluorophores which were bound to the *b* subunit (Cy5 crosslinking the two *b* subunits at residue 64) and to one *c* subunit at the loop between the two transmembrane helices. These independent FRET measurements confirmed the existence of small rotary steps of *c* during ATP synthesis as well as hydrolysis. The model for the rotary catalysis in the F_0 part of ATP synthase by a stepwise transfer of protons between subunits *a* to *c* in a sequential one-by-one mode appears to be correct.

2.4 Hidden Markov Models to identify rotational movements

New tools to get objective classifications of FRET states and transitions are required because the primary step of single-molecule FRET trajectory analysis by manual assignment is always questionable. More generally, extracting levels and transitions between levels in noisy data is the scientific challenge. Solutions to tackle these problems exist, which can be modified and applied to the FRET trajectory analysis. We started to develop a Hidden-Markov-Model-based software to automatically extract FRET levels, transitions and dwell times from single-molecule data [23, 9].

The basis of a general Markov model is a number of states q_i which a system can adopt, that is, a number of orientations of the rotor subunits in a single F_0F_1 -ATP synthase. The length of the state is the dwell time of the rotor in a particular orientation. For a Markov state, the dwell time distribution is purely monoexponential and is determined by a single probability value. Markov states are independent from the past states. In a system with N states, there are $N \cdot (N-1)$ independent state transitions forming the transition probability matrix K . In a *hidden* Markov system the states themselves are not directly observable, but emit a random variable x_t (i.e. FRET efficiency) with a characteristic probability density function for each state q_i . This is the so-called emission function $f_i(x|q_i)$. In general, the unequivocal back-assignment from x to q is not possible which makes the actual states to hidden states.

The temporal evolution of a Hidden-Markov-Model (HMM) is a chain of hidden states, i.e. a sequence of orientations of the rotor subunits, and a trajectory of observables (FRET efficiency trajectory from fluorescence intensities of FRET donor and acceptor fluorophores) linked *via* the emission function. An example of a hidden Markov model is shown in Fig. 3a. Dwell times and transitions between the states are described by rate constants. For each state a distribution of observables is given as Gaussians (Fig. 3b). A measured data point at $x=0.35$ can be related to all three states; however, the probability to originate from hidden state 2 is much higher than from 1 or 3.

The goal is to infer from the trajectory of observables to all system parameters of the HMM. The central component in this process is the loglikelihood function, $\log L$, which comprises the mean value of state q , the covariance of state q , and the occurrence of state q . The loglikelihood function yields a probability prediction of the system parameter set given the measured FRET data. Finding the appropriate values for the parameters is therefore a optimization problem which can be solved by multi dimensional optimization algorithms. We use the HMM Matlab-toolbox of K. Murphy and develop new maximum-likelihood estimators for the mean value and the covariance of a state. Thus we can account for the fluorescence intensity fluctuations within a single

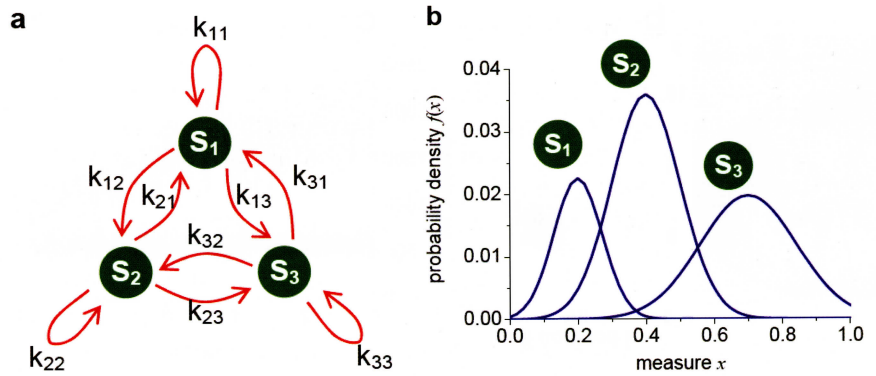


Fig. 3: (a) Scheme of a Markov Model with three states S_1 , S_2 , and S_3 and their corresponding transition probabilities k_{ij} . (b) Three Gaussian emission functions with different means μ , variances Σ and occurrences W ($\mu_{q=1,3}=0.2, 0.4, 0.7$; $\Sigma_{q=1,3}=0.005, 0.01, 0.02$; $W_{q=1,3}=0.20, 0.45, 0.35$). For the FRET-labeled F_0F_1 -ATP synthase, the Gaussians approximate the distribution of FRET efficiencies to each particular orientation of the rotor subunit.

photon burst due to the Brownian motion of the singly reconstituted F_0F_1 -ATP synthase in the laser focus.

We applied a three-state HMM to the three-stepped rotation of the ϵ subunit in F_0F_1 -ATP synthase during ATP hydrolysis[9]. In comparison to the manual analysis of FRET transitions, the same three FRET levels were found by the HMM; also the transition rates supported the manually assigned dwell times. In the presence of the non-competitive inhibitor aurovertin B, the dwell times were prolonged during ATP hydrolysis. This indicates the hindered conformational dynamics of the β subunits as expected from the binding site of aurovertin B on the moving domain of β . In addition, we have used the HMM analysis to prove the 36° step size of the c ring in F_0F_1 -ATP synthase during ATP synthesis. Given five hidden states for FRET symmetry reasons of the c ring, the HMM recovered the orientations of the c -ring with respect to the a subunit and attributed the dwell times in the range of 6 to 10 ms similarly to the manually assigned FRET levels.

2.5 Prolonged observation times with the ABEL trap

One principal drawback of the confocal FRET analysis of freely diffusing enzymes is the limited observation time in the laser focus. For nanotechnological applications, a localized ATP source is preferred to power biological linear motors. However, we could not mount the liposomes with F_0F_1 -ATP synthase to a modified glass surface without losing the activity of the enzyme, that is, we found only reduced reactivity and low turnover numbers for these enzymes.

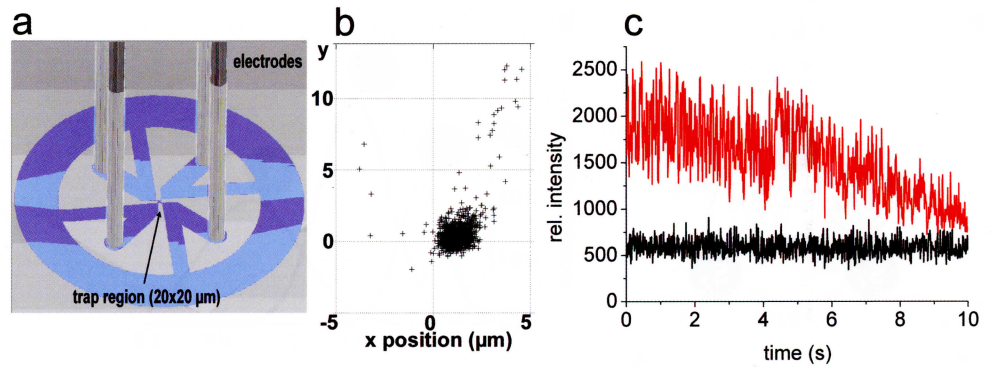


Fig. 4: The ABEL trap. (a) Design with four Pt-electrodes. The trap region is located in a flat region in middle of the four channels. (b) Positions of an ABEL-trapped single liposome labeled with rhodamine B. The liposome escapes from the ABEL trap after photobleaching of nearly all rhodamines. (c) Fluorescence intensity trajectories of this liposome at the target position (red trace) and of the background (black trace).

Accordingly, we evaluated three-dimensional trapping methods for a single proteoliposome in solution.

The optical trap made of an NIR laser focus can attract large liposomes or micrometer-sized polystyrene beads. However, in order to trap small liposomes with diameters of 100 nm the laser power has to increase to more than 100 mW, which might result in a local rise of the temperature. Comparison of rotational motion monitored by single-molecule FRET and biochemical turnover rates require appropriate temperature controls. In addition, the high NIR laser power in the trapping focus will enhance photobleaching of the two single reporter fluorophores in the FRET experiment.

An alternative way to trap small particles like viruses or liposomes in solution is the “Anti-Brownian electrokinetic trap” (ABEL trap) developed by A. E. Cohen and W. E. Moerner[24–26]. A fast feedback from the optical positioning signal is applied to four electrodes in a two-dimensional microfluidic device (Fig. 4a). The trapping region within the microfluidics made from the polymer PDMS on a waver stamp has a size of $20 \times 20 \mu\text{m}$ in x-y dimensions and is about $1 \mu\text{m}$ deep. Depending on the distance to a given x-y target position, the electrode potentials cause electrophoresis plus an electric field gradient resulting in a transport of the particle to the set point. Thus, Brownian motion of a single nanoparticle can be compensated.

We develop the ABEL trap concept in collaboration with A. E. Cohen and W. E. Moerner towards monitoring FRET changes in single F_0F_1 -ATP synthase, that is, for subunit rotation by FRET. Therefore, lipids of the proteoliposomes are labeled additionally with an NIR dye and are observed by a fast CCD camera

in the microfluidic device. The set point for the feedback is the confocal laser spot for the F_0F_1 -ATP synthase FRET measurement. Using an intensified CCD camera we have built an ABEL trap and were able to hold liposomes labeled with rhodamines (Fig. 4b,c) or oxazine dyes like 'Atto680'. Liposomes with a diameter of 100–150 nm were confined to ± 500 nm for more than 10 seconds at camera frame rates of 100 Hz. This is sufficient to observe sequences of many full rotations in a trapped F_0F_1 -ATP synthase.

3 Conclusions

F_0F_1 -ATP synthase is a unique rotary double motor which can be used for multiple purposes in nanotechnology. Making ATP for other biological transport systems is a biomimetic approach which requires membrane-embedded enzymes and an electrochemical potential difference of protons across the lipid membrane. This difference can be controlled by nanoelectrochemistry using the nanometer-sized tip of a small platinum electrode for local water oxidation or reduction. While generating H_2 or O_2 on one electrode, protons or OH^- remain and change the pH. Because biological systems need buffered solutions, the higher concentrations of protons or OH^- is restricted to the vicinity of the tip by the chemical lens effect of the surrounding buffer[27] (Fig. 5).

To address the single F_0F_1 -ATP synthase for ATP production, the liposomes have to be bound to a solid support (Fig. 5) or trapped three-dimensionally in solution. Thus, we will evaluate the fastest version of the ABEL trap with apparently no detectable deviation from the target point, which can be combined with a confocal FRET microscope to monitor rotation.

The F_1 motor can be used to sense the local ATP concentration by a rotation read-out. The measurement principle could be based on video microscopic observations of rotation using attached polystyrene beads, ultrastable fluorophores[28] or fluorescent nanocrystals. Because long observation times in the range of hours are needed, new non-bleaching fluorescent markers have to be used.

A promising new fluorophore is the fluorescent nitrogen-vacancy color center (NV) in diamonds. NV centers are absolutely photostable with a quantum yield of nearly 100% and show no blinking behaviour[29–31]. Fluorescent nanodiamonds with diameters smaller than 5 nm have been produced and used for single-molecule tracking in life cells[32]. The surface of the nanodiamonds can be modified by silane chemistry. Thus, nanodiamonds can be attached to the F_0F_1 -ATP synthase[33] as shown for the quantum dots. Using a non-fluorescent quencher QSY21 directly bound to the diamond surface decreased the fluorescence lifetime of a single defect center paving the way

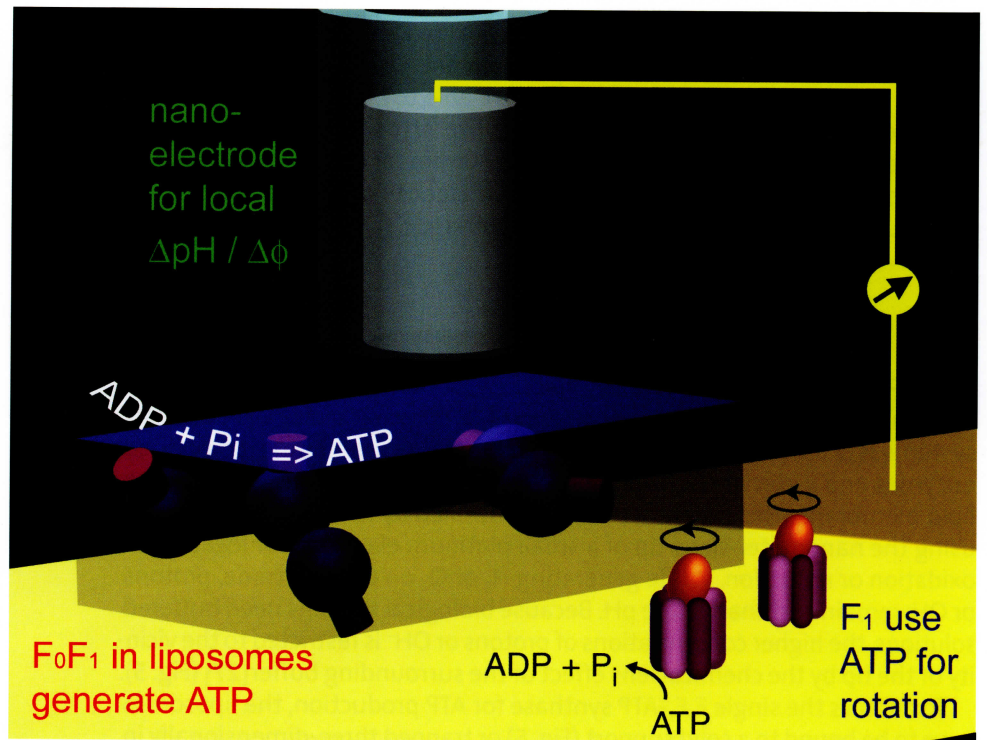


Fig. 5: Scheme for the nanotechnological application of F_0F_1 -ATP synthase as a switchable localized ATP source. The enzymes are embedded in liposomes (blue balls) and positioned in a porous matrix. To initiate and control ATP synthesis, the nanoelectrode is used for electrochemical OH^- production. Surface-bound F_1 motors with fluorescent nanoparticles attached to the rotary γ subunit act as ATP sensors using the rotational speed as the read-out for the ATP concentration.

for single-molecule FRET measurements with ultrastable nanocrystals as FRET donors. In addition, in combination with small quantum dots emitting around 530 nm, the NV centers in nanodiamond can act as the FRET acceptor to yield an ultrastable new FRET pair to study the rotational movements of the biological nanomotor and ATP producer F_0F_1 -ATP synthase.

Acknowledgements

The authors want to thank the members of the research groups at the Universities of Freiburg and Stuttgart as well as the collaborators for their exceptional contributions to the success of this interdisciplinary work. We are grateful for the financial support from the Baden-Württemberg Stiftung in the network of competence "Functional Nanostructures".

References

- [1] B. Bottcher, I. Bertsche, R. Reuter, and P. Graber. *Direct visualisation of conformational changes in EF(0)F(1) by electron microscopy*, J. Mol. Biol. **296**, 449 (2000)
- [2] S. Steigmiller, P. Turina, and P. Graber. *The thermodynamic H⁺/ATP ratios of the H⁺-ATP synthases from chloroplasts and Escherichia coli*, Proc. Natl. Acad. Sci. USA **105**, 3745 (2008)
- [3] P.D. Boyer. *The ATP synthase – a splendid molecular machine*, Annu. Rev. Biochem. **66**, 717 (1997)
- [4] Y. Sambongi, Y. Iko, M. Tanabe, H. Omote, A. Iwamoto-Kihara, I. Ueda, T. Yanagida, Y. Wada, and M. Futai. *Mechanical rotation of the c subunit oligomer in ATP synthase (FOF1): direct observation*, Science **286**, 1722 (1999)
- [5] W. Junge, H. Sielaff, and S. Engelbrecht. *Torque generation and elastic power transmission in the rotary FOF1-ATPase*, Nature **459**, 364 (2009)
- [6] M. Diez, B. Zimmermann, M. Borsch, M. König, E. Schweinberger, S. Steigmiller, R. Reuter, S. Felekyan, V. Kudryavtsev, C.A. Seidel, and P. Graber. *Proton-powered subunit rotation in single membrane-bound FOF1-ATP synthase*, Nat. Struct. Mol. Biol. **11**, 135 (2004)
- [7] B. Zimmermann, M. Diez, N. Zarrabi, P. Graber, and M. Borsch. *Movements of the epsilon-subunit during catalysis and activation in single membrane-bound H⁽⁺⁾-ATP synthase*, EMBO J. **24**, 2053 (2005)

- [8] M.G. Duser, Y. Bi, N. Zarrabi, S.D. Dunn, and M. Borsch. *The proton-translocating a subunit of F₀F₁-ATP synthase is allocated asymmetrically to the peripheral stalk*, The Journal of biological chemistry **283**, 33602 (2008)
- [9] K.M. Johnson, L. Swenson, A.W. Pipari, Jr., R. Reuter, N. Zarrabi, C.A. Fierke, M. Borsch, and G.D. Glick. *Mechanistic basis for differential inhibition of the F₁F₀-ATPase by aurovertin*, Biopolymers **91**(10), 830–840 (2009)
- [10] H. Noji, R. Yasuda, M. Yoshida, and K. Kinosita, Jr. *Direct observation of the rotation of F₁-ATPase*, Nature **386**, 299 (1997)
- [11] Y. Zhou, T.M. Duncan, V.V. Bulygin, M.L. Hutcheon, and R.L. Cross. *ATP hydrolysis by membrane-bound Escherichia coli F₀F₁ causes rotation of the gamma subunit relative to the beta subunits*, Biochimica et biophysica acta **1275**, 96 (1996)
- [12] K. Hasler, S. Engelbrecht, and W. Junge. *Three-stepped rotation of subunits gamma and epsilon in single molecules of F-ATPase as revealed by polarized, confocal fluorometry*, FEBS letters **426**, 301 (1998)
- [13] R. Yasuda, H. Noji, M. Yoshida, K. Kinosita, Jr., and H. Itoh. *Resolution of distinct rotational substeps by submillisecond kinetic analysis of F₁-ATPase*, Nature **410**, 898 (2001)
- [14] T. Elston, H. Wang, and G. Oster. *Energy transduction in ATP synthase*, Nature **391**, 510 (1998)
- [15] A. Aksimentiev, I.A. Balabin, R.H. Fillingame, and K. Schulten. *Insights into the molecular mechanism of rotation in the F₀ sector of ATP synthase*, Biophys. J. **86**, 1332 (2004)
- [16] M. Borsch, M. Diez, B. Zimmermann, R. Reuter, and P. Graber. *Stepwise rotation of the gamma-subunit of F₀F₁-ATP synthase observed by intramolecular single-molecule fluorescence resonance energy transfer*, FEBS letters **527**, 147 (2002)
- [17] M.G. Duser, N. Zarrabi, Y. Bi, B. Zimmermann, S.D. Dunn, and M. Borsch. *3D-localization of the a-subunit in F₀F₁-ATP synthase by time resolved single-molecule FRET*, Proc. SPIE **6092**, 60920H (2006)

- [18] M. Borsch, M. Diez, B. Zimmermann, M. Trost, S. Steigmiller, and P. Graber. *Stepwise rotation of the gamma-subunit of EFoF1-ATP synthase during ATP synthesis: a single-molecule FRET approach*, Proc. SPIE **4962**, 11 (2003)
- [19] N. Zarrabi, M.G. Duser, S. Ernst, R. Reuter, G.D. Glick, S.D. Dunn, J. Wrachtrup, and M. Borsch. *Monitoring the rotary motors of single FoF1-ATP synthase by synchronized multi channel TCSPC*, Proc. SPIE **6771**, 67710F (2007)
- [20] E. Galvez, M. Duser, M. Borsch, J. Wrachtrup, and P. Graber. *Quantum dots for single-pair fluorescence resonance energy transfer in membrane-integrated EFoF1*, Biochem. Soc. Trans. **36**, 1017 (2008)
- [21] E.M. Galvez, B. Zimmermann, V. Rombach-Riegraf, R. Bienert, and P. Graber. *Fluorescence resonance energy transfer in single enzyme molecules with a quantum dot as donor*, Eur. Biophys. J. Biophys. **37**, 1367 (2008)
- [22] M.G. Düser, N. Zarrabi, D.J. Cipriano, S. Ernst, G.D. Glick, S.D. Dunn, and M. Borsch. *36° step size of proton-driven c-ring rotation in F_oF₁-ATP synthase*, EMBO J. **28**(18), 2689–2696 (2009)
- [23] N. Zarrabi, M.G. Duser, R. Reuter, S.D. Dunn, J. Wrachtrup, and M. Borsch. *Detecting substeps in the rotary motors of FoF1-ATP synthase by Hidden Markov Models*, Proc. SPIE **6444**, 64440E (2007)
- [24] A.E. Cohen. *Control of nanoparticles with arbitrary two-dimensional force fields*, Phys. Rev. Lett. **94**, 118102 (2005)
- [25] A.E. Cohen and W.E. Moerner. *The anti-Brownian electrophoretic trap (ABEL trap): fabrication and software*, Proc. SPIE **5699**, 296 (2005)
- [26] A.E. Cohen and W.E. Moerner. *Suppressing Brownian motion of individual biomolecules in solution*, Proc. Natl. Acad. Sci. USA **103**, 4362 (2006)
- [27] F.M. Boldt, J. Heinze, M. Diez, J. Petersen, and M. Borsch. *Real-time pH microscopy down to the molecular level by combined scanning electrochemical microscopy/single-molecule fluorescence spectroscopy*, Anal. Chem. **76**, 3473 (2004)

- [28] K. Peneva, G. Mihov, A. Herrmann, N. Zarrabi, M. Borsch, T.M. Duncan, and K. Mullen. *Exploiting the Nitrilotriacetic Acid Moiety for Biolabeling with Ultrastable Perylene Dyes*, *J. Am. Chem. Soc.* **130**, 5398 (2008)
- [29] G. Balasubramanian, I.Y. Chan, R. Kolesov, M. Al-Hmoud, J. Tisler, C. Shin, C. Kim, A. Wojcik, P.R. Hemmer, A. Krueger, T. Hanke, A. Leitenstorfer, R. Bratschitsch, F. Jelezko, and J. Wrachtrup. *Nanoscale imaging magnetometry with diamond spins under ambient conditions*, *Nature* **455**, 648 (2008)
- [30] J.-P. Boudou, P.A. Curmi, F. Jelezko, J. Wrachtrup, P. Aubert, M. Sennour, G. Balasubramanian, R. Reuter, A. Thorel, and E. Gaffet. *High yield fabrication of fluorescent nanodiamonds*, *Nanotechnology* **20**, 235602 (2009)
- [31] J. Tisler, G. Balasubramanian, B. Naydenov, R. Kolesov, B. Grotz, R. Reuter, J.-P. Boudou, P.A. Curmi, M. Sennour, A. Thorel, M. Börsch, K. Aulenbacher, R. Erdmann, P.R. Hemmer, F. Jelezko, and J. Wrachtrup. *Fluorescence and Spin Properties of Defects in Single Digit Nanodiamonds*, *ACS Nano* **3**(7), 1959–1965 (2009)
- [32] F. Neugart, A. Zappe, F. Jelezko, C. Tietz, J.P. Boudou, A. Krueger, and J. Wrachtrup. *Dynamics of diamond nanoparticles in solution and cells*, *Nano Letters* **7**, 3588 (2007)
- [33] M. Borsch, R. Reuter, G. Balasubramanian, R. Erdmann, F. Jelezko, and J. Wrachtrup. *Fluorescent nanodiamonds for FRET-based monitoring of a single biological nanomotor F₁-ATP synthase*, *Proc. SPIE* **7183**, 71832N (2009)